

Empirical mode decomposition: a novel technique for the study of tremor time series

Eduardo Rocon de Lima · Adriano O. Andrade ·
José Luis Pons · Peter Kyberd · Slawomir J. Nasuto

Received: 4 November 2005 / Accepted: 21 April 2006 / Published online: 20 June 2006
© International Federation for Medical and Biological Engineering 2006

Abstract Tremor is a clinical feature characterized by oscillations of a part of the body. The detection and study of tremor is an important step in investigations seeking to explain underlying control strategies of the central nervous system under natural (or physiological) and pathological conditions. It is well established that tremorous activity is composed of deterministic and stochastic components. For this reason, the use of digital signal processing techniques (DSP) which take into account the nonlinearity and nonstationarity of such signals may bring new information into the signal analysis which is often obscured by traditional linear techniques (e.g. Fourier analysis). In this context, this paper introduces the application of the empirical mode decomposition (EMD) and Hilbert spectrum (HS), which are relatively new DSP techniques for the analysis of nonlinear and nonstationary time-series, for the study of tremor. Our results, obtained from the analysis of experimental signals collected from 31 patients with different neurological conditions, showed that the EMD could automatically decompose acquired signals into basic components, called intrinsic

mode functions (IMFs), representing tremorous and voluntary activity. The identification of a physical meaning for IMFs in the context of tremor analysis suggests an alternative and new way of detecting tremorous activity. These results may be relevant for those applications requiring automatic detection of tremor. Furthermore, the energy of IMFs was visualized as a function of time and frequency by means of the HS. This analysis showed that the variation of energy of tremorous and voluntary activity could be distinguished and characterized on the HS. Such results may be relevant for those applications aiming to identify neurological disorders. In general, both the HS and EMD demonstrated to be very useful to perform objective analysis of any kind of tremor and can therefore be potentially used to perform functional assessment.

Keywords Tremor · Empirical mode decomposition · Inertial sensors · Tremor quantification · Tremor diagnostic · Time–frequency analysis · Hilbert spectrum

E. R. de Lima (✉) · J. L. Pons
Instituto de Automática Industrial, Carretera Campo Real,
km 0.200, La Poveda—Arganda del Rey,
28500 Madrid, Spain
e-mail: erocon@iai.csic.es

A. O. Andrade · S. J. Nasuto
University of Reading, Reading, UK

P. Kyberd
University of New Brunswick, Fredericton, NB, Canada

1 Introduction

Tremor is a rhythmic, involuntary muscular contraction characterized by oscillations of a part of the body [6]. Although the most common types of tremor have been subject of numerous studies, their mechanisms and origins are still unknown [16, 19, 25].

Neurological disorders associated with aging are often accompanied by tremor, which can affect various parts of the body such as hands, head, facial structures, tongue, trunk, and legs. Although the disorder is not

life-threatening, it can be responsible for functional disability and social embarrassment [12]. It is well established that tremorous activity is composed of deterministic and stochastic components [28].

The detection and quantification of tremor are of clinical interest for diagnosis of neurological disorders and objective evaluation of their treatment [15, 25, 27]. Methods based on the Fourier transform (FT) are commonly employed for this purpose, specially because of the similarity between the tremor to a sine wave [11]. For instance, the weighted Fourier linear combiner (WFLC) [24] characterizes the tremor based on its approximation by a sinusoidal waveform. Another example is the extraction of frequency parameters from the power spectrum (based on the FT) of the tremor for classification purposes [9–12, 25].

Some inherent drawbacks of techniques based on the FT are pointed out in [1, 2]. First, the signal is *linearly* decomposed as combination of sines and cosines. Second, the compromise between time and frequency resolution of methods based on the FT may not highlight the presence of local oscillations in the signal which can have important physical meaning.

In order to overcome some of the limitations of the FT, a number of approaches have been proposed and used. Among them, the use of parametric analysis methods, such as autoregressive (AR) models have been successfully applied to the power spectrum estimate of distinct biological signals [1]. The AR power spectrum estimate involves estimating the model parameters, referred to as AR coefficients. The definition of the number of AR coefficients (model order) and also the selection of a technique (e.g. Yule-Walker and Burg methods [1]) for their estimation influence over the characteristics of the power spectrum. Furthermore, it has been shown [1] that in some applications, for instance, in the analysis of heavily noise-corrupted signals AR models may not be suitable for an adequate signal modeling.

Recently, a novel technique for analysis of nonlinear and nonstationary time-series was successfully applied to investigations of seismological and biological signals [3, 4, 17]. This technique was first introduced in [18], and it is formed by two complementary tools, which are called empirical mode decomposition (EMD) and Hilbert spectrum (HS). The EMD decomposes any arbitrary time-series into a set of components designated as intrinsic mode functions (IMFs). The main aim of the EMD is to iteratively identify distinct time-scales (or frequency bandwidths) from the data that may have a physical meaning, e.g. IMFs may be related to biological phenomena. The existence of such a meaning is not guaranteed and an important issue in

any practical investigation applying this technique is to define or identify it [18].

Once IMFs are extracted from the signal it is possible to analyze how their energy evolves as a function of time and frequency on the HS. In contrast to the spectrogram (based on the FT) the HS is a windowing independent time–frequency representation that may provide enough resolution in the signal analysis for detection of events often obscured in a conventional analysis. Examples showing the gain in resolution provided by the HS when compared to the spectrogram and scalogram (wavelets) are given in [3, 17, 18].

This paper introduces the application of the EMD and HS as an alternative tool to the study of tremor. First we show that in this context, IMFs have a physical meaning, that is, single IMFs may represent either voluntary or involuntary movement activity of patients. The identification of such a physical meaning for IMFs is relevant because it shows that the method can automatically detect tremor. Note that the automatic detection of tremor is an important stage in systems that aim to control limb oscillations, and also in biofeedback studies. Second, we show that other physiological events that normally accompany the tremor, e.g. spasms, may also be identified in some IMFs.

In a further analysis we employ the HS to visualize how the energy of IMFs varies as a function of time and frequency. This study showed that the energy of voluntary and involuntary movement activity could be well distinguished on the HS. This result may be useful for investigations that aim to classify distinct neurological disorders, as the precise characterization of the energy of abnormal oscillations in limbs is a crucial stage in these studies. Our results are based on an extensive analysis of signals collected from 31 subjects suffering from distinct neurological disorders and executing different types of movements or tasks.

2 The Hilbert spectrum

The generation of the HS is performed in two steps. First, the EMD decomposes the input time-series into a set of functions designated as IMFs, and second those functions are used for generation of a 3-D plot called the HS.

2.1 The Empirical mode decomposition

The main aim of the EMD is to decompose a time-series into a set of components or functions known as

IMFs. This class of function was defined by Huang et al. [18]. To be considered as an IMF a time-series has to satisfy two conditions: first, in the whole data set, the number of extrema and the number of zero crossings must be either equal or differ at most by one, and second, at any point, the mean value of the envelope defined by the local maxima and the envelope defined by the local minima is zero.

Note that the decomposition of a time-series into IMFs consists in the identification of the basic units (IMFs) in that time-series. A practical procedure, known as sifting process, is employed for this purpose. It involves the following steps, leading to a decomposition of the signal $S(t)$ into its constituent IMFs:

1. x (an auxiliary variable) is set to the signal to be analyzed and a variable k , which is the number of estimated IMFs, is set to zero.
2. Splines are fitted to the upper extrema and the lower extrema. This will define the lower (LE) and upper envelopes (UE).
3. The average envelope, m , is calculated as the arithmetic mean between UE and LE.
4. A candidate IMF, h , is estimated as the difference between x and m .
5. If h does not fulfill the criteria defining an IMF, it is assigned to the variable x and the steps 2–4 are repeated. Otherwise, if h is an IMF then the procedure moves to step 6.
6. If h is an IMF it is saved as c_k , where k is the k th component.
7. The mean squared error, MSE, between two consecutive IMFs c_{k-1} and c_k , is calculated, and this value is compared to a stopping condition (usually a very small value, i.e. 10^{-5}).
8. If the stopping condition is not reached, the partial residue, r_k , is estimated as the difference between a previous partial residue r_{k-1} and c_k , and its content is assigned to the dummy variable x and the steps 2–4 are repeated.
9. If the stopping condition is reached then the sifting process is finalized and the final residue r_{final} can be estimated as the difference between $S(t)$ and the sum of all IMFs.

Note that the criterion used to state whether h is an IMF or not is to verify if h satisfies the two conditions that define an IMF.

An important feature of the sifting process is that it, adaptively and based solely on the data, is able to find appropriate time-scales that may reveal important information embedded in the original signal. In fact, single IMFs may have a physical meaning (i.e. may be related to a biological phenomenon), and as already

highlighted an important issue in any practical application is to determine the existence of this meaning.

2.2 Hilbert spectrum generation

Once IMFs are obtained as a result of the sifting process, it is possible to generate the HS, or a 3-D plot (time–frequency–energy) that represents the variation of frequency and energy of IMFs over time. The notion of frequency and energy for each IMF is obtained by employing the concept of analytic signals.

An analytic signal is a complex signal with one-sided spectrum that preserves all information contained in the original signal [21]. Note that the representation of a real signal as an analytical signal eliminates redundancy, since the negative half of the signal frequency spectrum containing redundant information with respect to the positive half is eliminated. A very simple way of estimating an analytical signal is by employing the Hilbert transform [8]. The real part of an analytical signal is the original input time-series, whereas its complex component is the Hilbert transform of that signal.

Given an analytic signal, $Z(t)$, defined as $Z(t)=X(t)+iY(t)=a(t) e^{j\theta(t)}$, where $X(t)$ is the input time-series and $Y(t)$ the Hilbert transform of $X(t)$, the following instantaneous attributes of $Z(t)$ can be defined:

$$a(t) = [X(t)^2 + Y(t)^2]^{1/2} \tag{1}$$

$$\theta(t) = \arctan\left(\frac{Y(t)}{X(t)}\right) \tag{2}$$

$$\omega(t) = \frac{d\theta(t)}{dt} \tag{3}$$

where $a(t)$ is the instantaneous amplitude, $\theta(t)$ is the instantaneous phase, and $\omega(t)$ is the instantaneous frequency.

With the definition of instantaneous attributes above the HS, $H(\omega,t)$, is generated as follows:

1. Estimate IMFs from the input signal.
2. Estimate the instantaneous attributes of each IMF.
3. Generate a 3-D plot, $H(\omega,t)$, in which the amplitude is contoured in the time–frequency plane.

In contrast to other time–frequency methods, the HS does not define an explicit equation that maps a 1-D time-series into a 3-D representation that provides information about time, frequency, and energy (amplitude).

From the HS it is also possible to estimate the marginal Hilbert spectrum (MHS), $h(\omega)$, which is defined in Eq. 4.

$$h(\omega) = \int_0^T H(\omega, t) dt \quad (4)$$

2.3 Comments

It is relevant to note that the EMD is responsible for estimating IMFs, which are a set of components in the time domain that represent embedded oscillations in the analyzed signal. The HS is a joint time–frequency representation obtained through the application of the Hilbert transform to IMFs. Therefore, the HS allows for visualization of the contribution and variation of the energy of all IMFs in a single plot. Such a representation may be useful for identification of events, represented by IMFs, not easily noted in the time domain. However, the EMD technique is completely independent of the HS and can have different applications, e.g. signal filtering [3].

Furthermore, it is possible to estimate the HS of any arbitrary time-series prior to its decomposition, however, in this case embedded oscillations in this signal will not be visualized on the HS, making it difficult to detect the presence of relevant physical events (e.g. oscillations that may be related to a biological event).

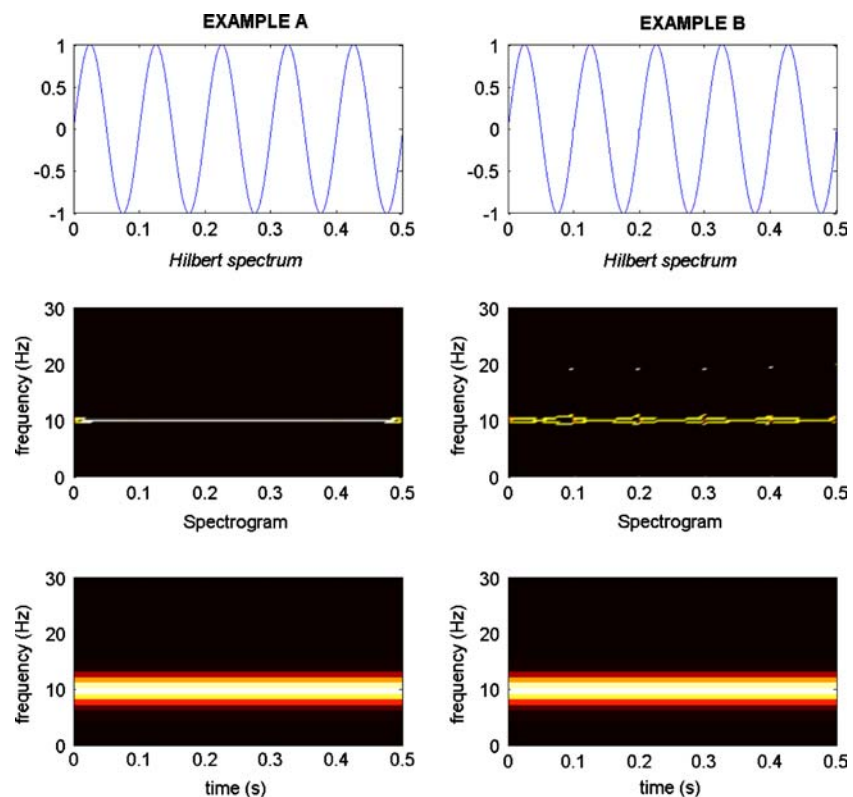
2.4 Calibration of the Hilbert spectrum and marginal Hilbert spectrum

In this section, a simple example regarding the analysis of a synthetic signal (sine wave) is employed to illustrate the application of the HS and MHS and also to compare this technique with those based on the FT. Further comparisons between HS and other time–frequency distributions through the investigation of artificial, electromyographic, and seismological signals are given in [3, 17, 18].

The frequency of oscillation of the sine wave was defined as $f_o=10$ Hz, and it lasted for $T=0.5$ s and was sampled at $F_s=1,000$ Hz. The HS and spectrogram of this signal are shown in Fig. 1 (Example A), and its MHS and power spectrum are presented in Fig. 2. In contrast to the HS and MHS, in both estimates the Fourier-based methods yielded energy spread around the actual frequency of oscillation of the signal (10 Hz).

In another example (see Fig. 1, Example B) some discontinuities lasting 1 ms, which may represent a failure in the analog-to-digital converter, were deliberately introduced in the signal shown in Fig. 1 (Example A). The resulting signal is shown in Fig. 1 (Example B). The visual inspection of this signal shows

Fig. 1 Example A: Hilbert spectrum and spectrogram of a sine wave oscillating at 10 Hz. Example B: Hilbert spectrum and spectrogram of a sine wave oscillating at 10 Hz with discontinuities at 0.1, 0.2, 0.3, and 0.4 s



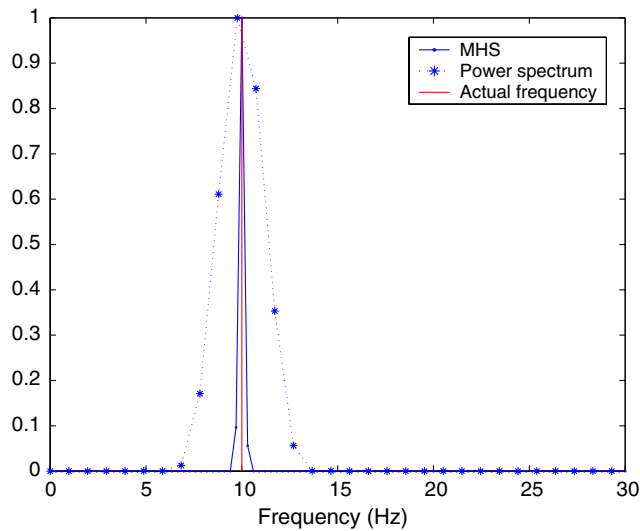


Fig. 2 Comparison between MHS and power spectrum estimated from the signal shown in Fig. 1 (Example A). The actual frequency of oscillation of this signal is marked with a *solid line* at 10 Hz

that the discontinuities cannot be visualized in time-domain, however they are clearly perceived on the HS (bright spots of energy around 0.1, 0.2, 0.3, and 0.4 s) and are not detected on the spectrogram because of the lack of resolution of this technique.

3 The experimental protocol

In order to assess tremor characteristics we studied its behavior in 31 patients suffering from different pathologies (Table 1). The average age of patients was 52.3 years old (ranging from 23 to 84 years old). All patients provided their written consent for the experiments.

The diagnosis of the condition of patients was given by the neurological staff of the General Hospital of

Table 1 Description of the type of disorders and tremors investigated. The way that patients expressed the tremor is also included, for instance, patients with essential disorder expressed the tremor during voluntary muscle contraction

Disorder	Type of tremor	Number of patients
Essential	Postural and kinetic	21
Cerebellar	Kinetic	4
Parkinson	Postural and rest	3
Patients with unclear tremor	Postural, kinetic and rest	3

Valencia (GHV, Spain) and the functional state of patients was evaluated by means of the Fahn scale [14]. Ethical approval for this research has been granted by the Ethical Committee of the GHV.

3.1 Sensors

There is a continuous need to develop miniaturized systems with low energy consumption for biomechanical analysis that can extract a wide range of parameters from human motion. Kinematic data obtained by biomechanical studies have been increasingly used and required in active prosthetics/orthotics control systems [26].

The tremor was detected by a customized sensor [22, 26], which is based on the combination of two independent gyroscopes placed distally and proximally to the joint of interest. The joint angular speed is obtained by subtraction of the angular speed measured by one gyroscope from the angular speed measured by the other one. The weight of the system is roughly 15 g [26], which is a low-mass system when compared to other sensors used in the field, for instance, Elble [13] employed a 15 g triaxial piezoresistive accelerometer secured to a 57 g plastic splint in his experiments. The use of a low-mass sensor is important to reduce the effect of low-pass filtering on the detected signal. Further discussion about this issue is presented in [13, 26].

This system could measure the upper limb joint angle, velocity and acceleration without any external reference. Unlike accelerometers, the measurement of angular velocity is not influenced by gravity and they are in general accurate both in frequency and amplitude.

The main advantages of this system are that it is light, cheap, and does not cause any discomfort to subjects thus providing a powerful tool to monitor biomechanical variables during physiological tremor movements.

3.1.1 Gyroscope placement

Since gyroscope provides absolute angular velocity in its active axis, the combination of two independent gyroscopes was used. They were placed distally and proximally to the joint of interest. Gyroscopes could be placed anywhere along the same plane on the same segment providing almost identical signals. The gyroscopes could therefore be attached to a convenient position in order to avoid areas of skin and muscle movement [30]. Figure 3 illustrates the placement of the gyroscopes.

With gyroscopes positioned as indicated in Fig. 3, the following movements of the upper limb were measured:

- Elbow flex-extension
- Forearm pron-supination
- Wrist flex-extension
- Wrist deviation

These articulations were selected because they are considered the most important articulations in the kinematic chain of the upper limb [20, 31].

3.2 Tasks

Six different tasks were employed for excitation of tremor. They are defined as follows:

1. Rest: The patient was asked to keep the arms in a rest position with the hands resting on the thighs (elbow flexed at 90° and the shoulder at 0° and hands in pronation).
2. Reaching for an object: Patients had to point at a target (at the shoulder height) located in front of them. They were asked to perform the movement slowly. The distance between the shoulder and the tip of the middle finger was 85% of upper limb length.
3. Drawing a spiral: The patient was asked to follow with the index finger a spiral drawn in a sheet of paper fixed in front of them.
4. Arm outstretched: The patient was asked to maintain the upper limbs outstretched in front of them, hands in supination, against the gravity, for 30 s.

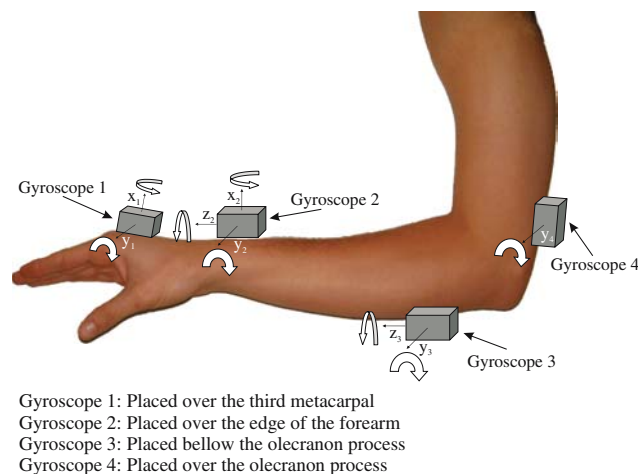


Fig. 3 Strategy for positioning of sensors on the upper limb of patients. The weight of the system is roughly 15 g and do not influence the tremorous movement of the patient

5. Touching nose: The patient was asked to touch the nose with the index finger, starting from a rest position (hand on the thigh). They had to keep the finger on the nose during 10 s.
6. Moving a cup: The patient was asked to take a rigid cup with one hand and move it to the left and to the right. They were sitting near to a white table. The target locations were identified by black tape fixed on the table. The tape was fixed along a line passing through positions defined as DEL and DER. The patient was first asked to maintain the elbow flexed at 90° and the shoulder at 0° , close to the trunk in the frontal plane. Hands were in pronation on the table with fingers extended. The targets were located at 10 cm on the left and on the right from the extremity of the third finger (DE left and DE right). Areas of the position of the cup were pre-drawn with a red marker.

In all tasks the patient was sitting on a chair. This set of tasks aims to activate all different types of tremor. Figure 4 illustrates a patient performing the six tasks presented above.

4 Data analysis

Figure 5 depicts the sequence of steps for data analysis. The resulting movement profile (or the collected signal x) was sampled at 400 Hz and filtered using a fifth order low-pass FIR filter with cutoff frequency set to 20 Hz. This is relevant for attenuation of the influence of any high-frequency noise on the digitized signal y .

In a further step, y was manually decomposed into tremor and voluntary activity by means of a digital pass-band Butterworth filter. Note that the word manually (or manual) in this paper refers to the ad hoc setting of the the cutoff frequencies of the digital filter in contrast to an automatic setting provided by adaptive methods like the EMD.

For estimation of the voluntary movement, VM_{ref} , the cutoff frequencies of this filter were set to 0–2 Hz. The cutoff frequencies employed for detection of the tremor, T_{ref} , were 2–20 Hz. Previous investigation of this data set showed that the tremor activity was limited between 3 and 8 Hz [7], and that voluntary movements were always below 2 Hz for the tasks described above. It is well established in the literature of tremor that the voluntary movement and tremor movement used to be separated in frequency. Tremor (2–12 Hz) tends to be at higher frequencies than voluntary (0–2 Hz) movements [12, 24]. Note that those digital filters do not introduce phase lag in the filtered signal.

Fig. 4 Tasks of the measurement session: **a** rest, **b** reaching for an object, **c** drawing spiral, **d** arm outstretched, **e** touching nose, **f** moving a cup

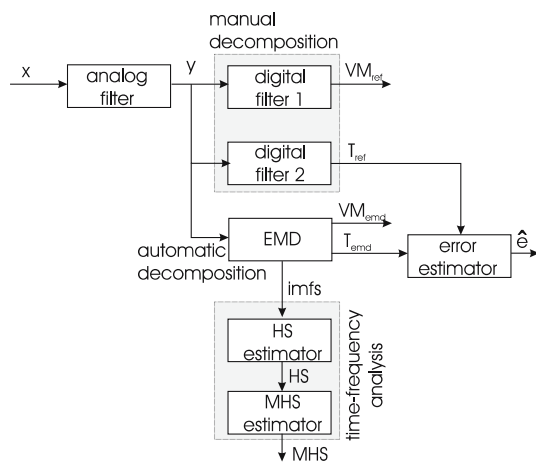
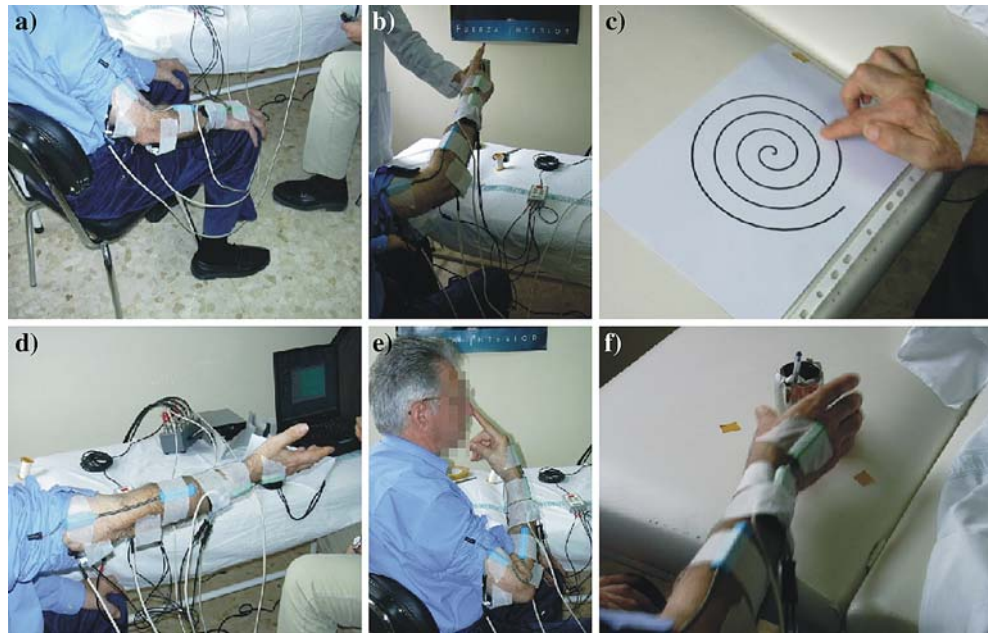


Fig. 5 Block diagram showing the sequence of analyses performed in this study. First the detected signal x was filtered and digitized in order to yield the time-series y . In a further step this signal was decomposed into tremor (T_{ref}) and voluntary movement (VM_{ref}). This was manually performed by means of two distinct digital filters. The same signal y was also automatically decomposed via EMD, and the automatically estimated tremor T_{emd} was compared to T_{ref} . The components provided by the EMD, or imfs, were employed for a further analysis of the signal y in the frequency domain

The time-series y was also automatically decomposed via EMD. This decomposition yielded IMFs from which it was possible to identify the tremor T_{emd} and voluntary movement VM_{emd} . A comparison between T_{emd} and T_{ref} was performed and resulted in the generation of the estimated square error signal $\hat{e} = \sqrt{(T_{ref} - T_{emd})^2}$. This signal measured the discrepancy between automatic and manual estimates.

A small value for \hat{e} indicates a strong relation between an IMF (T_{emd}) and a manual definition of tremor (T_{ref}). Thus, in practice, a small \hat{e} is a good evidence that T_{emd} has a physical meaning related to tremor activity. The identification of such a physical meaning is the main focus in this paper.

An additional investigation showing how the activities of tremor and voluntary movement were perceived in the frequency domain was also performed. For this purpose, the HS and MHS were employed as indicated in Fig. 5.

Figure 6 shows an example of a signal manually decomposed into its constituents, i.e. the voluntary movement and tremor.

5 Results

5.1 Automatic detection of tremor

The signal presented in Fig. 7 (top) was detected from a patient with essential tremor performing the draw spiral test. The signal components, or IMFs, obtained by means of the EMD are also shown in this figure. The first component identified as IMF_1 is the finest time-scale component, whereas the last component (IMF_4) is the largest time-scale component.

A comparative study between different IMFs and the tremor signal (obtained manually) showed that the IMF_1 , which is the component that best represents the high frequencies of the signal, was an accurate estimate of the tremor, i.e. this component had a very strong

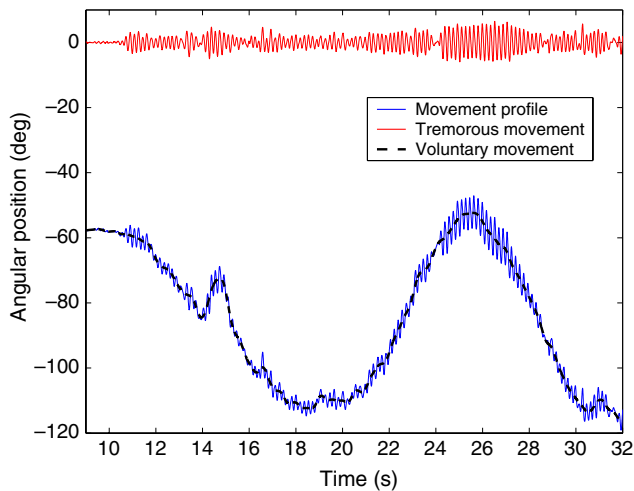
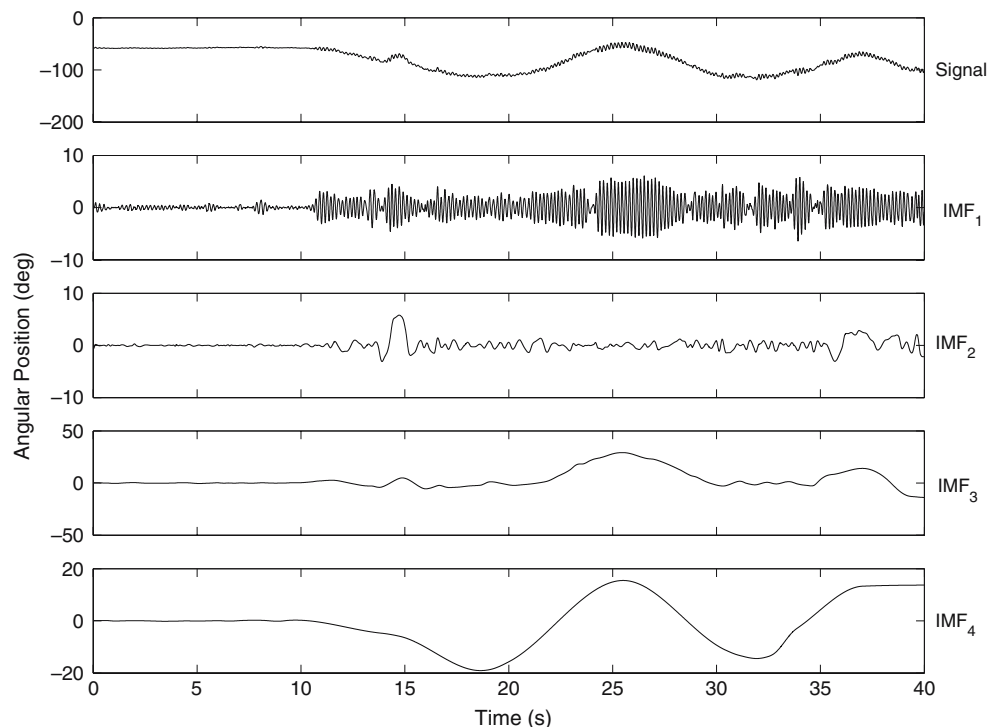


Fig. 6 Example of a manual decomposition of the movement profile (x) of an essential tremor patient performing the task of drawing a spiral. Digital filters are employed for estimation of tremulous movement (T_{ref}), oscillating around zero in the top, and voluntary movement (VM_{ref})

physical meaning. This observation is illustrated in Fig. 8. The manual estimate of the tremor is in the top of the figure, its automatic estimate, or IMF_1 , is in the middle, and the estimated error, $\hat{\epsilon}$, between those two signals is shown in the bottom. Note that the error is very small.

The same analysis for the signal in Fig. 7 was carried out for all available data sets. It was also noted that the

Fig. 7 Decomposition of a movement profile (signal) detected from an essential tremor patient provided by EMD. Four intrinsic mode function (IMF_1, \dots, IMF_4) were obtained. IMF_1 was identified as the tremulous movement



voluntary movement can be obtained by the summation of all available IMFs but the first one, which represented the tremor (see Fig. 9).

This investigation showed that the first IMF was always a precise estimate of the tremor. This accuracy was quantified by the mean square error signal, $\bar{\epsilon} = \text{mean}(\hat{\epsilon})$. The average and standard deviation of distinct signal errors $\bar{\epsilon}$ was estimated. The results show that a very small error, $0.09 \pm 0.19^\circ$, was obtained for all pathologies. Note that due to the fact that majority of patients suffers from essential tremor the results are only representative for the tremor activity related to this pathology. Nevertheless, the results indicate that the method is able to estimate tremor activity for all pathologies evaluated. Additional investigation should be pursued in order to validate the performance of this technique in the estimation of tremorous movements from other pathologies.

5.2 Visualization of tremor on the Hilbert spectrum

It has been shown that a particular intrinsic function is physically related to the tremor. Besides the representation of embedded components in the signal those functions may also be employed for a time–frequency analysis of time-series. This is obtained via the HS.

In practice it was observed that the HS could describe the variation of the energy and frequency of tremor and voluntary movement activities distinctly.

Fig. 8 Comparison between IMF_1 (from Fig. 7) and the manual estimate of the tremor (T_{ref}). Note that the error signal is very small

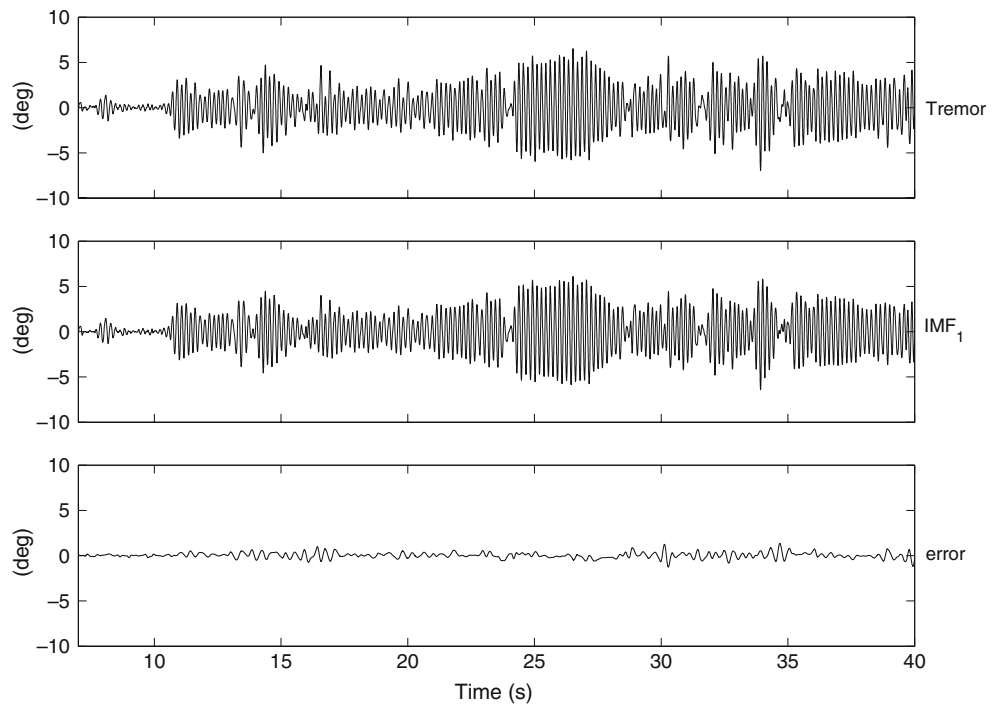
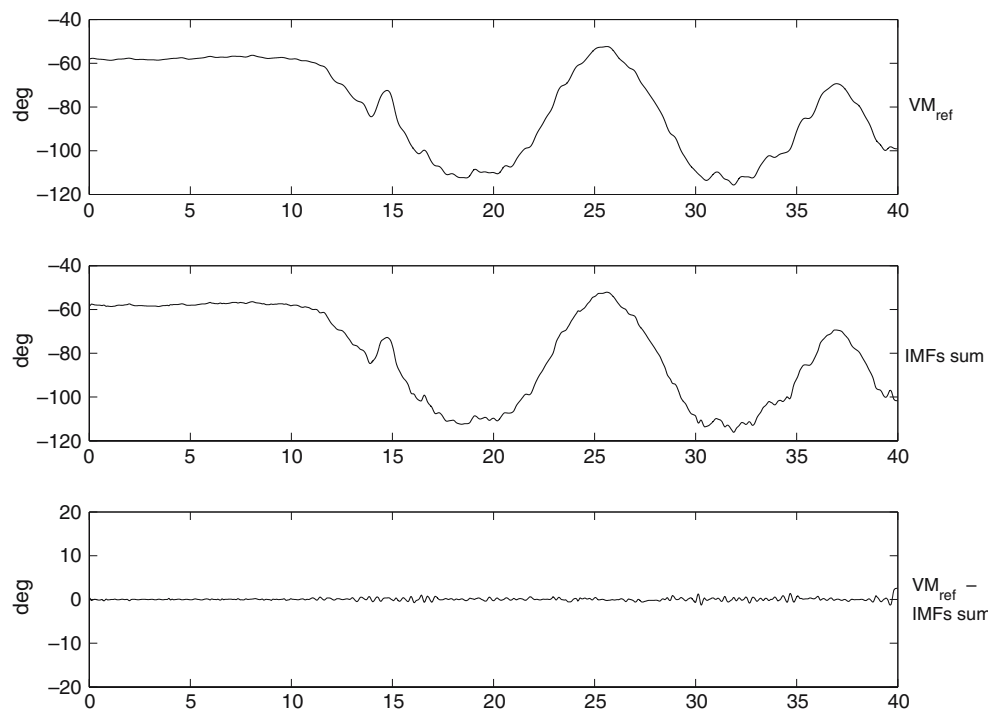


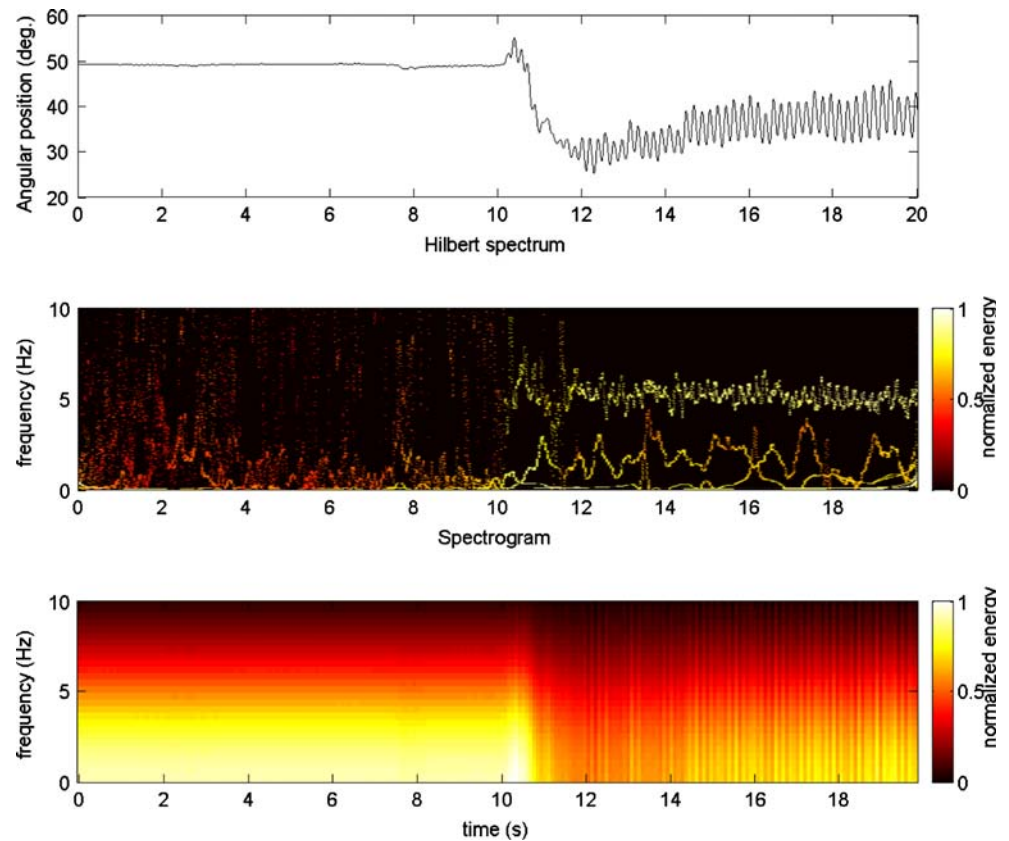
Fig. 9 Comparison between voluntary motion (*top*) and its estimate obtained via summation of different IMFs (IMF_2, IMF_3, IMF_4) (*middle*) shown in Fig. 7. Note that the difference between the manual and the automatic estimation of the voluntary movement ($V_{ref} - IMF_s$ sum) is very small (*bottom*)



That is, the energy of tremor and voluntary movement was very well localized in time and frequency. This is illustrated in Figs. 10 and 11 for patients with different disorders. The oscillations around 5 Hz are related to tremor activities whereas the others are related to other components of the global movement.

In these figures, the spectrogram was also included for comparison with the HS. From their analysis it is possible to conclude that the spectrogram allows for a global description of the energy of the signal, whereas the HS provides information about local changes of energy over time.

Fig. 10 Hilbert spectrum and spectrogram of an essential tremor patient performing the task of keeping the arms outstretched. Note that the energy of the involuntary movement is clearly separated from the energy of the voluntary movement on the HS. This separation is not so evident on the spectrogram. The high levels of energy activity on the HS could be perceived when the patient is performing the task



5.3 Analysis of the power based on the marginal Hilbert spectrum

The integration of HS over time results in the MHS. The MHS describes how the signal energy varies as a function of the frequency. Solid line of Fig. 13 shows the MHS for a patient with essential tremor performing the task of touching the nose. Note that the distribution provided by the MHS is bimodal and that its first peak is related to the voluntary movement, whereas the second is the energy of tremor activity.

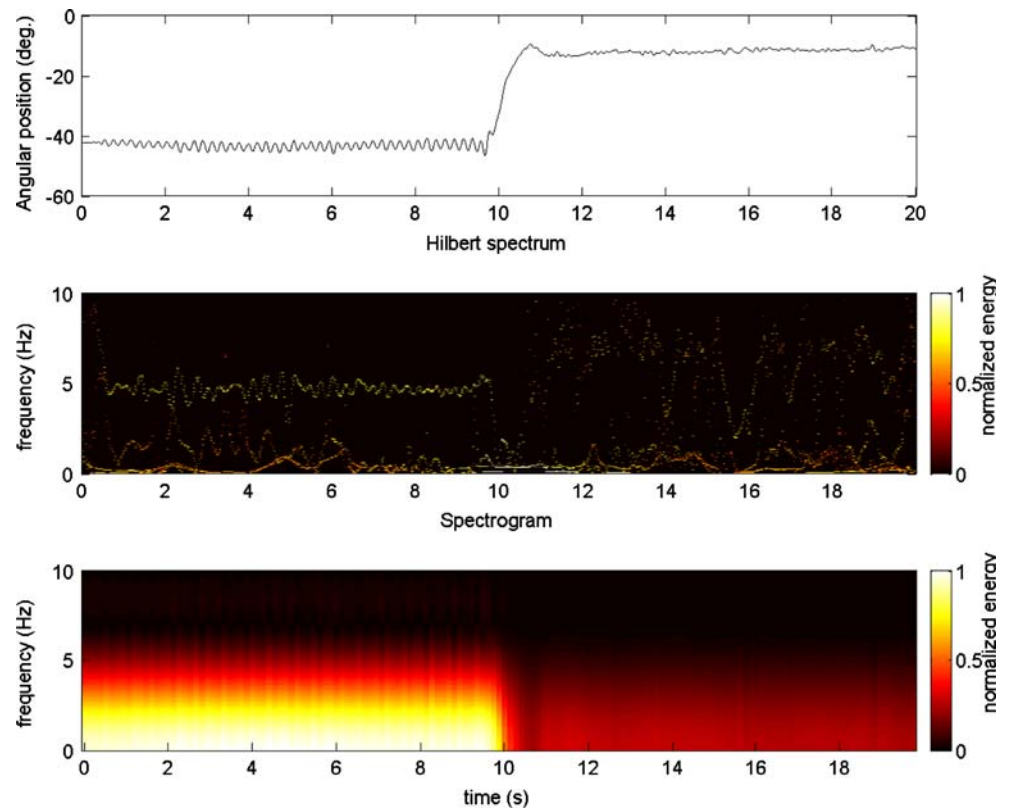
6 Discussion

In this section, an analysis of the results of the above proposed methodology is reported. We mainly focus on the application of EMD as a new tool for the study of tremor time series. EMD has been identified as a very useful tool for an automatic decomposition of the signal into tremor and voluntary signal. The results presented in this paper showed that the first IMF could accurately estimate the tremor. This was observed in the whole data set, which had more than 2,000 samples of signals with tremor activity, collected from 31 patients performing six different tasks.

Currently, there is no available technique that can accurately model the tremor [25, 29]. Most of the methodologies are based on the assumption that the tremor is stationary or is similar to sine wave. The fact that the tremor time series could be described by an IMF states that the tremor signal, for all patients considered in this study, satisfies two conditions [18]: (1) in the whole data set, the number of extrema and the number of zero crossings must be either equal or differ at most by one; (2) at any point, the mean value of the envelope defined by the local maxima and the envelope defined by the local minima is zero. These observations suggest that any investigation concerning the modeling of tremor should take into account those properties.

The major discrepancies between the signal estimated by EMD (IMF_1) and the tremor manually decomposed (T_{ref}) were found in the patients with unclear tremors. This may be explained by the fact that in those patients the movement profile was also corrupted by other involuntary movements besides tremor, such as spasms. A spasm is a sudden, involuntary contraction of a muscle or a group of muscles. Spasmodic muscle contraction may be due to a large number of medical conditions, including pathologies of the central nervous system, likely originating in those

Fig. 11 Hilbert spectrum and spectrogram of a Parkinson tremor patient performing the task of reaching for an object. The spectrogram could not show local variation of energy. Note that different from the HS presented in Fig. 10 the energy of the tremor is concentrated when the limbs are at rest, or within the first 10 s. This is a characteristic of Parkinsonian patients



parts of the brain concerned with motor function, such as the basal ganglia. For this reason it is very common that a number of patients affected by tremor also present spasmodic activity [23]. Spasms are a non-tremorous type of involuntary movement aperiodic, erratic, unpredictable at our current state of understanding, and can overlap in frequency with voluntary motion [23]. These movements can occur at higher frequencies overlapping the tremor frequency. In addition, these involuntary movements present an unstable and non-stationary behavior. This highlights the fact that in practice, any manual or arbitrary decomposition based on pre-fixed band-pass filters might result in an inaccurate estimate of the tremor movement or any other relevant physiological event (e.g. spasms), see Fig. 7.

In order to provide further evidence regarding the accuracy of the EMD in the estimate of tremorous movement an additional experiment was carried out. The first IMF was compared with the raw signal with tremorous activity obtained from the patient at rest. This signal was detected from a parkinsonian patient because in this condition the tremorous movement occurred when the patient had his arms at rest with the hands resting on the thighs, i.e no voluntary movement existed. The results of this experiment are shown in

Fig. 12. In the top of this figure the original signal is shown. In the middle, the EMD estimate for the tremor is presented, and in the bottom the square error between those signals is depicted. This result not only demonstrated the accuracy of the EMD estimate of the tremorous movement, but also supported the idea that the main source of error in the automatic estimate of tremor is due to the manual decomposition process (based on pre-fixed band-pass filters) used as reference.

A more detailed analysis of the IMF components indicates that the second IMF could estimate non-tremorous type of involuntary movements, such as spasms, [23], see Fig. 7 where the spasm movement present at time $t=15$ s is highlighted in the IMF_2 . The automatic identification of these movements is very important in order to help their understanding, as to date there is no technique able to identify these movements [5]. Further investigation correlating the signal provided by EMD estimation of spasmodic movements and EMG signals from the muscles that execute these movements will be carried out in order to validate this supposition.

Having obtained the IMF components, the Hilbert transform can be applied to each component and the instantaneous frequency can be computed, according to Eqs. 1–3. The HS enables the representation of the

amplitude and the instantaneous frequency of the input signal as a function of time in which the amplitude could be contoured on the time–frequency plane. Since the tremorous movements are well described by the first IMF, this method is a very useful tool for visualization of energy activity of tremor.

The description of the energy of the tremor on the HS is important because it allows for a good visualization of how the frequency and energy of the tremor vary over time. With this tool it is possible to clearly identify the onset and offset of tremor activity, as well as its frequency and amplitude changes over the time (see Figs. 10, 11). These techniques could be very useful to perform objective measurements of any kind of tremor and can therefore be used to perform tremor functional assessment.

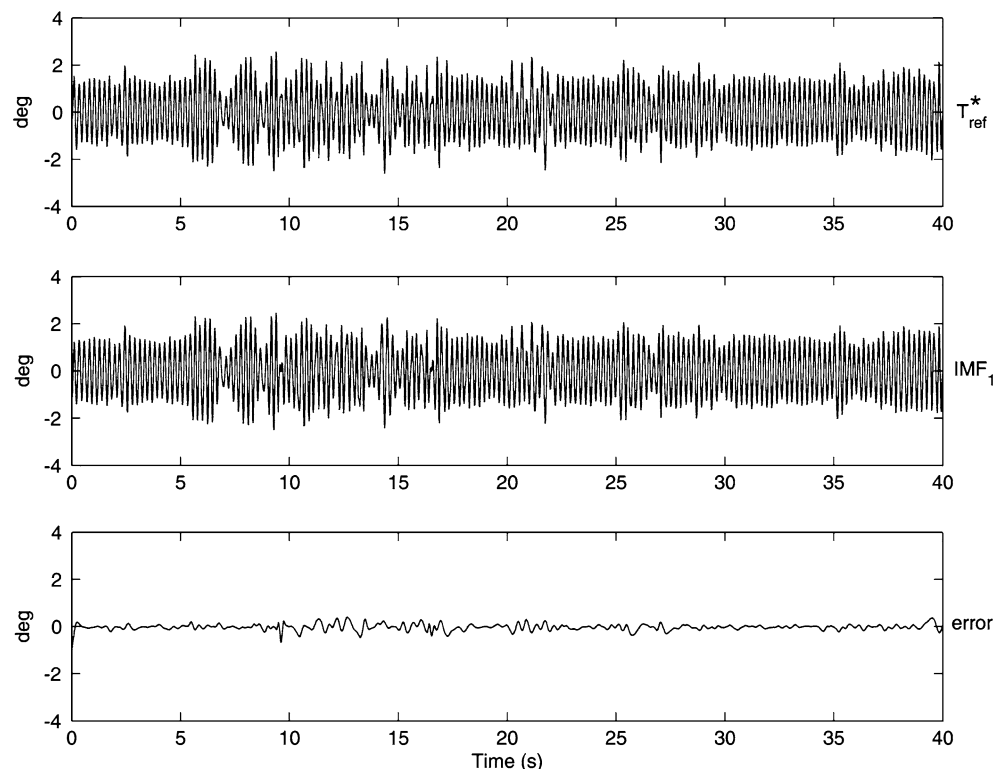
Due to its oscillatory characteristic, tremor is well suited to spectral analysis such as the FT, which is the most popular method of tremor quantification [25]. FFT-based spectral methods model the input signal as stationary periodic signal. Yet tremor amplitude and frequency are time-varying [11, 12, 24, 25], and therefore it is desirable to develop quantitative methods which do not assume stationarity. The MHS offers a measure of the total amplitude (or energy) contribution from each frequency value over the entire data span being able to precisely detect the energy activities of tremor and voluntary movements. In the Fourier

representation, the existence of energy at a frequency, ω , means a component of a sine or a cosine wave persisted through the time span of the data. Here, the existence of energy at a frequency, ω , means only that, in the whole time span of data, there is a greater likelihood for such wave to have appeared locally. Figure 13 shows a comparison between the Fourier spectrum and the MHS. It is clear that the MHS gives us a more precise spectrum, i.e. without energy spreading. In this example, a digital high-pass band filter with cutoff frequency set at 0.1 Hz, was employed for attenuating the very low frequency components of the signal. These components could obscure the interpretation of the FT power spectrum. The comparison between the MHS and the FT power spectrum shows that both techniques are able to localize high levels of energy below 1 Hz, and between 4 and 7 Hz. However, in this example the FT power spectrum shows higher spectral variation. Akay [1] showed, through the analysis of synthetic signals, that this energy variation may be related to spurious information introduced by the technique.

7 Conclusion

This paper introduced EMD as a novel tool for analysis of tremor time series. The main advantage of this

Fig. 12 Comparison between tremulous activity (T_{ref}^*), detected from a parkinsonian patient executing no voluntary movement, with the automatic estimate provided by the EMD (IMF_1). The square error between those signal is shown in the *bottom*



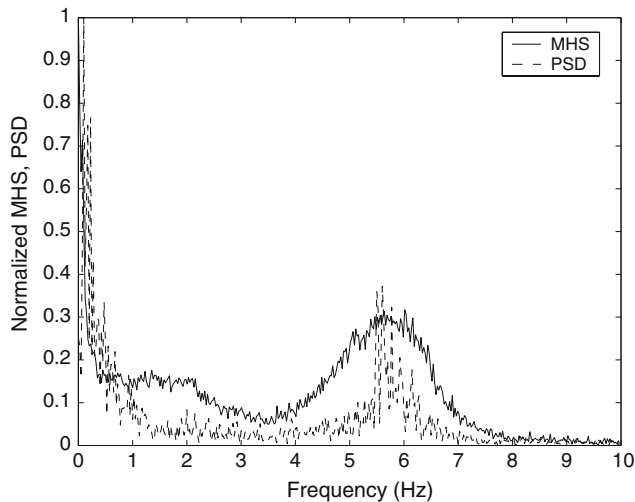


Fig. 13 Comparison between power spectrum based on the Fourier transform with the marginal Hilbert spectrum (MHS) estimated from the signal in Fig. 10 detected from an essential tremor patient performing the task of keeping the arms outstretched

technique is that it allows an automatic estimate of the tremorous movement in the different pathologies considered in this paper. Additional investigation should be pursued in order to validate the performance of this technique in the estimation of tremorous movements from other pathologies.

The authors believe that there is an evidence that EMD could identify other types of involuntary movements besides tremor, such as spasms. Nevertheless, this hypothesis should be validated by means of future investigation correlating involuntary movement activity and EMG signals from the muscles involved in generating these movements.

The technique presented is a high-resolution method that may be used as an alternative to Fourier-based analysis, which is the standard technique to the study of tremor time series. However, a detailed comparative study considering the HS and other joint time–frequency distributions (e.g. spectrogram, scalogram, autoregressive models, Wigner–Ville distribution) should be performed, in the study of tremor, to better understand the advantages and disadvantages of these techniques. Independent of such a study this research has shown that the HS has a promising application in the analysis of tremor.

The application of this technique introduces new attributes to the tremorous signal such as instantaneous amplitude, instantaneous phase, and instantaneous frequency. These attributes open the research field in the tremor field. Future work will be focused on the use of these parameters as parameters for the diagnosis of tremor pathologies.

References

1. Akay M (1994) Biomedical signal processing, 1st edn. Academic, Sandiego
2. Akay M (1999) Detection and estimation methods for biomedical signals. Academic, San Diego
3. Andrade AO (2005) Decomposition and analysis of electromyographic signals. PhD thesis, University of Reading, Reading
4. Andrade AO, Kyberd PJ, Taffler SD (2003) A novel spectral representation of electromyographic signals. In: Leder RS (ed) Engineering in medicine and biology society—25th annual international conference, Cancun, Mexico, vol 1, IEEE, pp 2598–2601
5. Ang WT (2004) Active Control compensation in Handheld Instrument for Microsurgery. PhD thesis, Johns Hopkins University
6. Anouti A, Koller W (1998) Tremor disorders: diagnosis and management. *West J Med* 162(6):523–530
7. Belda-Lois JM, Sanchez-Lacuesta J, Vivas-Broseta MJ, Ricon E, Bueno L, Pons JL (2003) Tremor movement analysis techniques: an approach towards ambulatory systems. *Assistive technology—shaping the future*, pp 827–831
8. Debnath L, Mikusinski P (1999) Introduction to Hilbert spaces with applications, 2nd edn. Academic, San Diego
9. Edwards R, Beuter A (1999) Using time domain characteristics to discriminate physiologic and parkinsonian tremors. *J Clin Neurophysiol* 17(1):87–100
10. Edwards R, Beuter A (1999) Using time frequency characteristics to discriminate physiologic and parkinsonian tremors. *J Clin Neurophysiol* 16:484–494
11. Elble RJ (1997) The pathophysiology of tremor. In: Watts RL, Koller WC (eds) *Movement disorders: neurologic principles and practice*. McGraw-Hill, New York, pp 405–417
12. Elble RJ, Koller WC (1990) Tremor. The Johns Hopkins University Press, Baltimore
13. Elble RJ (2003) Characteristics of physiologic tremor in young and elderly adults. *Clin Neurophysiol* 114:624–635
14. Fahn S, Tolosa E, Marin C (1998) Clinical rating scale for tremor. In: Tolosa E, Jankovic J (eds) *Parkinson's disease and movement disorders*. Urban & Schwarzenberg, Baltimore
15. Gantert C, Honerkamp J, Timmer J (1992) Analysing the dynamics of tremor time series. *Biol Cybern* 66:479–484
16. Gao JB, Wen-wen T (2002) Pathological tremors as diffusional processes. *Biol Cybern* 86:263–270
17. Huang NE, Chern CC, Huang K, Salvino LW, Long SR, Fan KL (2001) A new spectral representation of earthquake data: Hilbert spectral analysis of station TCU129, Chi-Chi, Taiwan, 21 September 1999. *Bull Seismol Soc Am* 91(5):1310–1338
18. Huang NE, Shen Z, Long SR, Wu MC, Shih HH, Zheng Q, Yen N-C, Tung CC, Liu HH (1998) The empirical mode decomposition and the Hilbert spectrum for nonlinear and non-stationary time series analysis. *Proc Roy Soc Lond* 454:903–995
19. Jain SS, Kirshblum SC (1993) Movement disorders, including tremors. In: Joel A, DeLisa JB (eds) *Rehabilitation medicine: principles and practice*, vol 2. Lippincott, Philadelphia
20. Kapandji IA (1983) The physiology of the joints: upper limb, vol 1. Churchill Livingstone, London
21. Marple LS Jr (1999) Computing the discrete-time “analytic” signal via fft. *IEEE Trans Signal Process* 47(9):2600–2603
22. Moreno JC, Freriks B, Thorsteinsson F, Sanchez J, Pons JL (2004) Intelligent knee–ankle–foot orthosis: the gait project approach. *Rehabilitation sciences in the new millennium—challenge for multidisciplinary research*, pp 271–274

23. Nechyba MC (1998) Learning and validation of human control strategies. PhD thesis, Johns Hopkins University, Baltimore
24. Riviere C (1981) Adaptive suppression of tremor for improved human-machine control. PhD thesis, Johns Hopkins University, Baltimore
25. Rocon E, Belda-Lois JM, Sanchez-Lacuesta JJ, Pons JL (2004) Pathological tremor management: modelling, compensatory technology and evaluation. *Technol Disabil* 16: 3–18
26. Rocon E, Ruiz AF, Pons JL (2005) On the use of rate gyroscopes for tremor sensing in the human upper limb. In: Proceedings of the international conference eurosensors XIX, p MP30
27. Timmer J, Gantert C, Deuschl G, Honerkamp J (1993) Characteristics of hand tremor time series. *Biol Cybern* 70:75–80
28. Timmer J, Haubler S, Lauk M, Lucking CH (1998) Pathological tremors: deterministic chaos or nonlinear stochastic oscillators? *Biol Cybern* 78:349–357
29. Timmer J, Lauk M, Deuschl G (1998) Cross-spectral analysis of physiological tremor and muscle activity. I. Theory and application to unsynchronized electromyogram. *Biol Cybern* 78:349–357
30. Tong K, Granat MH (1999) A practical gait analysis system using gyroscopes. *Med Eng Phys* 21:87–94
31. Viosca E, Peydro MF, Puchol A, Soler C, Prat J, Corts A, Sanchez J, Belda JM, Lafuente R, Poveda R (1999) Gufa de uso y prescripci=n de productos ortoprofTsicos a medida. IBV—Instituto Biomecánico de Valencia